A lack of classical Cepheids in the inner part of the Galactic disc

Noriyuki Matsunaga,[1][*] Michael W. Feast,[2,3] Giuseppe Bono,[4,5] Naoto Kobayashi,[6,7,8] Laura Inno,[9] Takahiro Nagayama,[10] Shogo Nishiyama,[11] Yoshiki Matsuoka[12] and Tetsuya Nagata[13]

[1]*Department of Astronomy, The University of Tokyo, 7-3-1 Hongo, Bunkyo-ku, Tokyo 113-0033, Japan*
[2]*Astrophysics, Cosmology and Gravity Centre, Astronomy Department, University of Cape Town, Rondebosch 7701, South Africa*
[3]*South African Astronomical Observatory, PO Box 9, Observatory 7935, South Africa*
[4]*Dipartimento di Fisica, Universitá di Roma Tor Vergata, Via della Ricerca Scientifica 1, I-00133 Rome, Italy*
[5]*Instituto Nazionale de Astrofisica, Osservatorio Astronomico di Roma, Via Frascati 33, I-00040 Monte Porzio Catone, Italy*
[6]*Institute of Astronomy, School of Science, The University of Tokyo, 2-21-1 Osawa, Mitaka, Tokyo 181-0015, Japan*
[7]*Kiso Observatory, Institute of Astronomy, School of Science, The University of Tokyo, 10762-30 Mitake, Kiso-machi, Kiso-gun, Nagano 397-0101, Japan*
[8]*Laboratory of Infrared High-Resolution Spectroscopy (LiH), Koyama Astronomical Observatory, Kyoto Sangyo University, Motoyama, Kamigamo, Kita-ku, Kyoto 603-8555, Japan*
[9]*Max Planck Institute for Astronomy, Königstuhl 17, D-69117 Heidelberg, Germany*
[10]*Department of Physics and Astronomy, Kagoshima University, 1-21-35 Korimoto, Kagoshima 890-0065, Japan*
[11]*Miyagi University of Education, Aoba-ku, Sendai, Miyagi 980-0845, Japan*
[12]*National Astronomical Observatory of Japan, 2-21-1 Osawa, Mitaka, Tokyo 181-8588, Japan*
[13]*Department of Astronomy, Kyoto University, Kitashirakawa-Oiwake-cho, Sakyo-ku, Kyoto 606-8502, Japan*

ABSTRACT

Recent large-scale infrared surveys have been revealing stellar populations in the inner Galaxy seen through strong interstellar extinction in the disc. In particular, classical Cepheids with their period–luminosity and period–age relations are useful tracers of Galactic structure and evolution. Interesting groups of Cepheids reported recently include four Cepheids in the nuclear stellar disc (NSD), about 200 pc around the Galactic Centre, found by Matsunaga et al. and those spread across the inner part of the disc reported by Dékány and collaborators. We here report our discovery of nearly 30 classical Cepheids towards the bulge region, some of which are common with Dékány et al., and discuss the large impact of the reddening correction on distance estimates for these objects. Assuming that the four Cepheids in the NSD are located at the distance of the Galactic Centre and that the near-infrared extinction law, i.e. wavelength dependency of the interstellar extinction, is not systematically different between the NSD and other bulge lines of sight, most of the other Cepheids presented here are located significantly further than the Galactic Centre. This suggests a lack of Cepheids in the inner 2.5 kpc region of the Galactic disc except the NSD. Recent radio observations show a similar distribution of star-forming regions.

Key words: stars: distances – stars: variables: Cepheids – dust, extinction – Galaxy: bulge – Galaxy: disc – infrared: stars.

1 INTRODUCTION

The structure of the inner Galaxy still remains to be revealed. While recent infrared surveys have led to discoveries of new features in the bulge (e.g. Nishiyama et al. 2005; Saito et al. 2011), the distribution of young stars, say younger than 1 Gyr, restricted to within a degree of the Galactic plane is still elusive. In addition to the strong foreground extinction towards the inner Galaxy, the high density of older stars in the bulge makes it difficult to trace the younger component(s).

It is therefore required to focus on some prominent tracers whose ages are easily deduced. For example, the nuclear stellar disc (NSD) has been long known to host massive stellar clusters whose ages are several Myr (Figer, McLean & Morris 1999; Figer et al. 2002). This stellar disc extends ∼400 pc around Sgr A* and co-exists with the massive reservoir of interstellar matter known as the Central Molecular Zone (Launhardt, Zylka & Mezger 2002). This region also hosts current star formation and young stellar objects spread across the NSD (Yusef-Zadeh et al. 2009; Mauerhan et al. 2010).

[*]E-mail: matsunaga@astron.s.u-tokyo.ac.jp

Classical Cepheids are also useful tracers of young stellar populations. They are pulsating supergiants with the famous period–luminosity relation (PLR) which enables us to estimate their distances reasonably well. They are evolved from intermediate-mass stars, 3.5–11 $M_{\odot}$, and their period–age relation allows us to trace stellar populations aged 10–300 Myr (Bono et al. 2005). Matsunaga et al. (2011) discovered three classical Cepheids in the NSD. The three Cepheids have similar periods, ∼20 d, which indicated that they are around 25 Myr old. Matsunaga et al. (2015), in addition to reporting another Cepheid with very similar characteristics, provided further support for the membership of the four Cepheids to the NSD based on radial velocities from near-infrared (IR) high-resolution spectra.

Dékány et al. (2015a,b) recently reported dozens of new Cepheids found in the VISTA Variables in the Vía Láctea (VVV) Survey (Minniti et al. 2010). Their new Cepheids are located towards the bulge region and more spread than the NSD, and Dékány et al. (2015b) concluded that they are in the inner part of the disc, within a few kpc around Sgr A*. Radio observations, however, do not support such ubiquitous distribution of young objects in the inner part of the disc. Recent deep radio observations have discovered two kinds of objects that trace star formation activities in the inner Galaxy: H ɪɪ regions detected in recombination line and radio continuum emission (e.g. Anderson et al. 2011, 2012), and maser spots in high-mass star-forming regions (e.g. Sanna et al. 2014). H ɪ absorption seen in the radio continuum of the former makes it possible to estimate locations of the H ɪɪ regions, while very long baseline interferometer observations of the latter, if conditions allow, enable one to obtain trigonometric distances. As discussed by Jones et al. (2013), no H ɪɪ regions have been identified within 4 kpc around Sgr A* except in the NSD, while at the edge of this void exist the expanding 3 kpc arms (Dame & Thaddeus 2008) with which H ɪɪ regions are associated.

In this paper, we report classical Cepheids newly discovered in our near-IR survey and discuss their distribution. In particular, we discuss the large effect of the extinction law. The ratio of total-to-selective extinction A_{K_s}/E_{H-K_s} is important, in our discussions, for estimating the extinction in K_s from the reddening in $H - K_s$. Nishiyama et al. (2006) obtained $A_{K_s}/E_{H-K_s} = 1.44 \pm 0.01$ based on their photometric data for red clump towards the bulge, while Nishiyama et al. (2009) combined the Two Micron All Sky Survey K_s magnitudes of red clump stars with the 2MASS colours of red giant stars in the same areas to obtain $A_{K_s}/E_{H-K_s} = 1.61 \pm 0.04$. This difference leads to estimates of extinction differing by ∼10 per cent; a smaller A_{K_s}/E_{H-K_s} value would result in a larger estimate of distance. Objects towards the Galactic Centre have large reddenings, 1.5–2.0 mag in E_{H-K_s}, thus leading to a large difference in distance moduli, 0.3–0.4 mag, which corresponds to 1.0–1.5 kpc at the distance of ∼8.0 kpc. Dékány et al. (2015a,b) adopted the A_{K_s}/E_{H-K_s} value from Nishiyama et al. (2009) after a transformation into their VVV photometric system, while adopting the smaller value from Nishiyama et al. (2006) would put their Cepheids further than they estimated as we discuss below in more detail.

2 OBSERVATION AND DATA ANALYSIS

Our observations were conducted using the Infrared Survey Facility (IRSF) 1.4-m telescope and the SIRIUS camera (Nagashima et al. 1999; Nagayama et al. 2003) which collects images in the J, H and K_s bands, simultaneously. These observations are thus on the same colour system as those of Nishiyama et al. (2006). The observed field is composed of 142 fields-of-view of IRSF/SIRIUS, covering

∼2.3 deg², between −10° and +10° in Galactic longitude along the Galactic plane, i.e. 0° in Galactic latitude. Observations at about 30 epochs were made between 2007 and 2012.

The basic data analysis was done in the same manner as in Matsunaga et al. (2009, 2013). In short, point spread function (PSF) fitting photometry was performed on every image using the ɪʀᴀꜰ/ᴅᴀᴏᴘʜᴏᴛ package, and variable stars were searched for by considering the standard deviations of time series photometric data. The variability search was done using the three-band data sets independently, so that we could find variables even if they are visible only in one of the JHK_s bands. In addition, we included the variable stars in Matsunaga et al. (2013) which are within the fields of this survey even if their variations are slightly smaller than the detection limits of variability. This survey is slightly shallower than that of Matsunaga et al. (2013), and as a result many objects are too faint to be detected in J band.

The saturation limits are 9.0, 9.0 and 8.5 mag in J, H and K_s, respectively. On the other hand, the detection limits vary across the survey region depending on the crowding. For example, the detection limits are 15.2, 14.9 and 14.1 mag for relatively sparse regions, $|l| > 8°$, while for crowded regions, $|l| < 1°$, they get shallower, 15.0, 14.1 and 13.0 mag in JHK_s. The definition of these limits is described in Matsunaga et al. (2009).

In this paper we use only H- and K_s-band magnitudes for estimating distances to Cepheids as done by Dékány et al. (2015a,b). We adopt the PLR of classical Cepheids from Matsunaga et al. (2013):

$$M(H) = -3.256(\log P - 1.3) - 6.562, \tag{1}$$

$$M(K_s) = -3.295(\log P - 1.3) - 6.685. \tag{2}$$

These relations were calibrated based on *Hubble Space Telescope* parallaxes of Cepheids in the solar neighbourhood (Benedict et al. 2007; van Leeuwen et al. 2007). These PLRs and the extinction coefficient of $A_{K_s}/E_{H-K_s} = 1.44$ (Nishiyama et al. 2006) are combined with observed magnitudes, H and K_s, to estimate the distance modulus μ_0 and the foreground extinction A_{K_s}.

3 RESULTS

We detected approximately 100 variable stars with period between 0.1 and 60 d, among which we identified 29 classical Cepheids (Table 1). We did not always detect the variables in all of the JHK_s bands; Table 1 includes Mflag which we also used in Matsunaga et al. (2013, 2015) to show the reasons of non-detection or the qualities of the listed magnitudes. All the objects we report here were detected in both H and K_s bands, while roughly half of them were too faint in the J band. Table 1 also lists A_{K_s} and μ_0 derived with H- and K_s-band mean magnitudes.

The short-period variables we detected include type II Cepheids and a few other types of variables like eclipsing binaries. We will describe details of the classification and results for other types in a forthcoming paper. The method of the classification is briefly given in Matsunaga (2014), but an important step is comparing their estimated distances and extinctions with a three-dimensional extinction map. With a given set of magnitude and colour, two types of Cepheids (classical and type II) would lead to significantly different distances, D, by a factor of ∼2, while the estimate of A_{K_s} is not largely affected thanks to the similarity of their period–colour relations. Thus, (D, A_{K_s}) in comparison with an extinction map along the line of sight allows us to determine the Cepheid type. We used the three-dimensional extinction map by Schultheis et al. (2014). Dékány et al. (2015a,b) used a similar method to

Table 1. Catalogue of classical Cepheids detected in our survey. After the numbering ID, the ID combining RA and Dec. (J2000.0) follows. Then listed are JHK_s mean magnitudes, amplitudes, Mflag, periods, distance moduli μ_0 and extinctions A_{K_s}. The mean magnitudes are intensity-scale means of maximum and minimum, and the amplitudes refer to peak-to-valley variations. The definition of the Mflag is given in Matsunaga et al. (2009).

No.	ID	J (mag)	H (mag)	K_s (mag)	ΔJ (mag)	ΔH (mag)	ΔK_s (mag)	Mflag	Period (d)	A_{K_s} (mag)	μ_0 (mag)
1	17201462−3711160	15.21	13.19	12.03	0.67	0.28	0.25	000	5.0999	1.53	15.24
2	17201826−3658528	15.22	12.83	11.54	0.38	0.27	0.18	000	9.944	1.70	15.53
3	17241258−3601469	13.66	11.58	10.46	0.38	0.34	0.35	000	17.597	1.44	15.53
4	17263471−3516241	–	13.65	11.80	–	0.35	0.27	300	13.405	2.50	15.42
5	17265423−3501081	–	15.98	13.99	–	0.67	0.37	360	4.2904	2.73	15.75
6	17295917−3409551	12.30	10.30	9.20	0.51	0.48	0.42	000	31.52	1.40	15.14
7	17321407−3323595	14.05	12.09	10.98	0.33	0.21	0.21	000	9.907	1.44	15.22
8	17384614−3126228	–	12.31	10.77	–	0.40	0.42	300	25.03	2.03	15.74
9	17404103−3041386	15.16	12.08	10.47	0.45	0.49	0.42	600	23.88	2.14	15.28
10	17445691−2913338	14.95	12.14	10.32	1.57	0.43	0.36	600	18.87	2.45	14.48
11	17453089−2903106	–	12.39	10.30	–	0.48	0.40	300	22.75	2.83	14.34
12	17453227−2902553	15.30	11.96	10.10	0.57	0.45	0.53	000	19.96	2.50	14.28
13	17460602−2846551	15.63	12.02	10.14	0.46	0.51	0.42	300	23.52	2.53	14.53
14	17494143−2727145	–	12.92	11.51	–	0.31	0.25	300	10.48	1.87	15.40
15	17501126−2719429	–	12.58	10.95	–	0.50	0.42	300	16.52	2.17	15.19
16	17503049−2713466	–	14.47	12.23	–	0.54	0.34	300	12.655	3.06	15.20
17	17511376−2648559	–	13.95	12.13	–	0.35	0.28	300	12.9488	2.45	15.74
18	17522166−2631194	–	14.25	12.27	–	0.35	0.27	300	11.9921	2.69	15.54
19	17522894−2623400	15.55	12.47	10.91	0.64	0.44	0.41	600	22.63	2.07	15.71
20	17523814−2619433	14.01	11.22	9.86	0.55	0.52	0.43	000	38.16	1.77	15.71
21	17544025−2534395	–	13.40	11.47	–	0.47	0.44	300	17.162	2.61	15.33
22	17573141−2430267	–	13.81	11.74	–	0.51	0.47	300	24.32	2.80	15.91
23	18012448−2254446	–	14.79	12.75	–	0.28	0.22	360	11.2397	2.77	15.84
24	18012508−2254283	–	14.85	12.73	–	0.56	0.32	360	11.2157	2.89	15.70
25	18021484−2227107	–	13.90	11.99	–	0.44	0.41	300	17.12	2.58	15.88
26	18032993−2203225	14.55	11.68	10.35	0.70	0.48	0.46	000	39.68	1.72	16.30
27	18035395−2158117	15.42	11.91	10.23	0.76	0.41	0.42	600	45.3	2.22	15.87
28	18055284−2106419	–	13.10	11.44	–	0.49	0.38	300	21.41	2.21	16.01
29	18070782−2034501	–	12.74	10.94	–	0.37	0.38	300	19	2.42	15.14

discriminate classical Cepheids from a large number of type II Cepheids in the bulge.

The extinction map depends on the extinction coefficient. Schultheis et al. (2014) used the extinction coefficient from Nishiyama et al. (2009) as done by Dékány et al., but their A_{K_s}/E_{H-K_s} is 1.63 considering the transformation from the 2MASS to the VVV system. The effect of this transformation, 0.02 in A_{K_s}/E_{H-K_s}, is negligible in the following discussions. Let us assume that an observed feature in the $(H - K_s)$–K_s diagram gives $A_{K_s} = 1.61$ at the distance of 8 kpc with $A_{K_s}/E_{H-K_s} = 1.61$ adopted, i.e. the observed reddening is 1 mag. If we adopted $A_{K_s}/E_{H-K_s} = 1.44$, the same feature would have $A_{K_s} = 1.44$ mag at the distance of 8.6 kpc. We transformed the extinction map by Schultheis et al. (2014) in this way, which typically reduced the A_{K_s} value of the original map by ∼10 per cent at each distance, and then compared the (D, A_{K_s}) curve with the parameters of our Cepheids. Such a change in the extinction map, however, did not affect our conclusion on Cepheid types because the predicted distances for the two types of Cepheids are significantly different compared to the effect of the extinction coefficient.

4 DISCUSSION

4.1 Comparison with Cepheids in Dékány et al. (2015a,b)

Dékány et al. (2015a,b) discovered 37 classical Cepheids from VVV (two in 2015a and 35 in 2015b). Among these objects, 11 are located within our survey region. Table 2 lists our objects which

Table 2. Matches in previous catalogues (a – Dékány et al. 2015a; b – Dékány et al. 2015b). The reference values of periods and JHK_s magnitudes are listed when available.

No.	Ref	ID	J (mag)	H (mag)	K_s (mag)	A_{K_s} (mag)	μ_0 (mag)
1	b	3	15.25	13.20	12.04	1.84	14.90
4	b	4	16.94	13.51	11.70	2.88	14.90
5	b	7	–	15.94	13.93	3.23	15.17
7	b	29	13.99	12.09	11.01	1.69	14.97
14	b	18	15.51	12.91	11.48	2.25	14.96
16	b	19	–	14.62	12.30	3.70	14.59
17	b	17	–	14.08	12.13	3.11	15.05
18	b	21	17.54	14.27	12.25	3.23	14.94
21	b	34	17.33	13.47	11.47	3.17	14.73
23	a	C1	19.13	14.76	12.71	3.27	15.27
24	a	C2	18.41	14.67	12.66	3.20	15.28

have counterparts in their catalogue together with the distances and reddenings they derived. All of them were detected in our survey although some of their light curves are rather noisy. Comparing A_{K_s} and μ_0 in Tables 1 and 2, we notice that significant differences, 0.25–0.7 mag, are present between the results in Dékány et al. (2015a,b) and ours.

The differences in the distance moduli, $\Delta\mu$, can be attributed to three reasons: measured magnitudes, the PLRs and the extinction law (Fig. 1). First, magnitudes of classical Cepheids in Tables 1 and 2 show significant scatter, ∼0.1 mag in H and ∼0.05 mag in
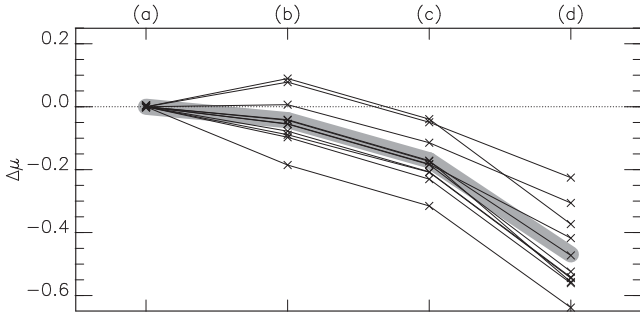
Figure 1. Distance moduli of 11 Cepheids, which were included in both Dékány's work and ours, are calculated with varying options of photometric data (either ours or those in Dékány et al. 2015a,b), the PLR (Monson et al. 2012 or Matsunaga et al. 2013) and extinction law (Nishiyama et al. 2006 or Nishiyama et al. 2009), and are compared with our values in Table 1. In the case of (a), our photometric data were used with our PLR (equations 1 and 2) and the extinction law of Nishiyama et al. (2006), which is our default analysis, and thus the offsets are zero. Dékány's photometric data were used in the case of (b). In the case of (c), furthermore, the PLR by Monson et al. (2012) were used. The extinction law was further changed to the N09 for (d). Grey thick line shows average offsets for the four cases.

K_s when compared with each other. This introduces a systematic offset of 0.04 mag in distance moduli with a standard deviation of 0.08 mag, which is illustrated by the (b) points in Fig. 1. While the differences in the photometric results produce the scatter of $\Delta\mu$, the systematic offset caused by this is not large.

The second cause of $\Delta\mu$ is the difference in the PLRs adopted. Dékány et al. (2015a,b) used PLRs by Monson et al. (2012) after the conversion of that photometric system to VISTA and the re-calibration of their zero-points based on the distance to the Large Magellanic Cloud (LMC), 18.493 mag in μ, obtained by Pietrzyński et al. (2013). Their PLRs are slightly different from the ones we adopted (equations 1 and 2). This leads to different estimates of distance modulus by 0.07–0.1 mag depending on $\log P$ of a Cepheid but independent of reddening; the PLRs by Monson et al. (2012) give smaller estimates of distance. As indicated by the (c) points in Fig. 1, this increases the systematic offset of $\Delta\mu$ to 0.17 mag.

Finally, the difference in the extinction coefficients adopted is the largest cause of the systematic offset. With E_{H-K_s} values of 1–2 mag given, the difference of 0.17 in A_{K_s}/E_{H-K_s} between Nishiyama et al. (2006) and Nishiyama et al. (2009) introduces offsets of 0.2–0.4 mag. Combining this with other offsets mentioned above, we can explain the large systematic offsets, $\Delta\mu \sim 0.47$ mag. This corresponds to ~1.7 kpc at the distance of 8 kpc.

Fig. 2 illustrates the effect of A_{K_s}/E_{H-K_s} on distances of Cepheids in this paper and those reported in Dékány et al. (2015a,b). The red curves in the upper panel corresponds to the results of four Cepheids (Nos 10–13 in Table 1) which we consider belong to the NSD. The horizontal line and shaded region indicate the recent estimate, 8.0 ± 0.5 kpc, of the Galactic Centre distance (Gillessen et al. 2013). The comparison between the distances of the four Cepheids and that of the Galactic Centre supports the coefficient of $A_{K_s}/E_{H-K_s} = 1.44$ or even smaller. The larger coefficient $A_{K_s}/E_{H-K_s} = 1.61$ would lead to significantly smaller distances of the four Cepheids, <7 kpc, which is rather unexpected as the distance to the NSD that is rotating around the Galactic Centre. The membership of these four Cepheids in the NSD seems secure. This is based on (1) their positions, (2) their closely similar distances (independent of the adopted reddening law), (3) their closely similar
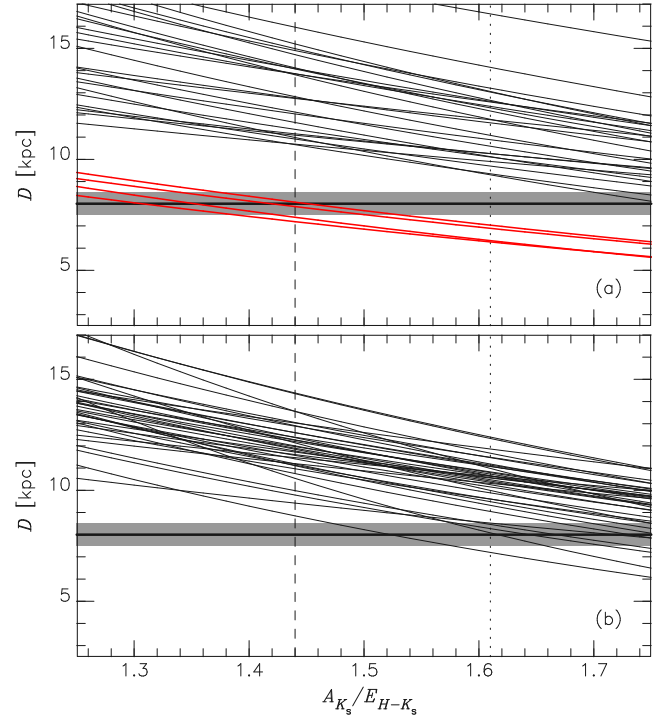

Figure 2. Variation of estimated distances of Cepheids plotted against the extinction coefficient A_{K_s}/E_{H-K_s}. The upper panel (a) is concerned with our Cepheids, while the lower panel (b) with those in Dékány et al. (2015a,b). The vertical lines mark the coefficients from Nishiyama et al. (2006, 2009). The horizontal line and grey area indicate the range of recent estimates of the Galactic Centre distance, 8.0 ± 0.5 kpc. Four Cepheids which are considered to be within the NSD, having $D \sim 8$ kpc with $A_{K_s}/E_{H-K_s} \sim 1.44$, are indicated by red curves.

periods (indicating an unusual period distribution and a significant increase in star formation ~25 Myr ago) and (4) their radial velocities which are consistent with orbits expected in the NSD. Full details of these aspects are given in Matsunaga et al. (2011, 2015). Therefore, we should use the smaller $A_{K_s}/E_{H-K_s} \sim 1.44$ at least for the four Cepheids towards the inner part of the bulge. In addition, Schödel et al. (2010) and Fritz et al. (2011) estimated A_{K_s}/E_{H-K_s} towards a small region around the Galactic Centre to be 1.30–1.35, even smaller than our value, which could put the average distance of the four NSD Cepheids closer to 8.0 kpc.

How about other Cepheids distributed between $\pm10°$ in Galactic longitude? The extinction law may be spatially variant. Nishiyama et al. (2006), for example, suggested a variation of ~0.1 in A_{K_s}/E_{H-K_s} towards different corners of the inner bulge, within 2°.5 around the Galactic Centre (also see Gosling, Bandyopadhyay & Blundell 2009; Chen et al. 2013; Nataf et al. 2013, concerning the spatial variation of the near-IR extinction law). If there were such variation, this would be the largest source of uncertainty in distances of the Cepheids discussed here. Nonetheless, if other Cepheids had similar distances to the four Cepheids at ~8 kpc, all of them should have large A_{K_s}/E_{H-K_s} values, 1.7 or more, which would be distinctly large compared to the value for the NSD objects. This is unlikely for the following reason. Several previous papers traced the shape of the Galactic bar using red clump distributed across a similar range of Galactic longitude, $|l| < 10°$ (Nishiyama et al. 2005; Rattenbury et al. 2007; Wegg & Gerhard 2013). Using a given extinction coefficient for the entire range of each study, the inclination of the bar appears as a smooth change of the peak distance of

the red clump. If the A_{K_s}/E_{H-K_s} towards the Central region were significantly different from other lines of sight, the bar structure in the above studies should have presented the effect of the systematic change instead of the smooth inclination. Therefore, we conclude that all the Cepheids in this study and Dékány et al. (2015a,b) are further than the four Cepheids in the NSD.

4.2 A lack of Cepheids in the inner part of the disc

In the following discussion, we use $A_{K_s}/E_{H-K_s} = 1.44$ for all of our Cepheids. In addition, we re-calculated the distances of the Cepheids reported by Dékány et al. (2015a,b) in the same way as for our Cepheids using the PLRs of equations (1) and (2) and the extinction law by Nishiyama et al. (2006). The distances and extinctions obtained are plotted in Fig. 3. The four Cepheids at around 8 kpc show a concentration to the value expected for objects in the Galactic Centre, while other objects show a wide range of (D, A_{K_s}) values at $D > 8$ kpc. The Cepheids from Dékány et al. (2015a,b) are now largely located behind the bulge. The revision of their distances does not change their distances from the Galactic plane so much, and they are within 50 pc of the plane except one, object 5 in Dékány et al. (2015b), being at ∼100 pc above the plane. Their locations are thus consistent with the thin disc behind the bulge.

From the magnitude range of our survey (Section 2) and the expected absolute magnitude, we can predict the range of (D, A_{K_s}) in which we can detect Cepheids. We here consider detections in both H and K_s, which are the most important bands in this study. Drawn in Fig. 3 are boundaries which correspond to the detection limits (dashed curves) and the saturation limits (solid curves) in the (D, A_{K_s}) plane. For each of the detection limits and the saturation limits, three curves are drawn for Cepheids with different periods, i.e. different absolute magnitudes. A Cepheid should have μ_0 and A_{K_s} which fall in between the corresponding dashed and
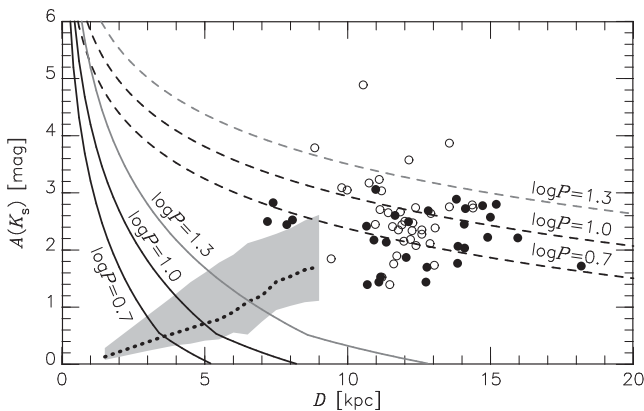

Figure 3. D and A_{K_s} of detected Cepheids are plotted – filled circles for our objects and open circles for those in Dékány et al. (2015a,b). Note that the reddening law by Nishiyama et al. (2006) was used for both sample in this plot. Also presented is the range of the (D, A_{K_s}) space in which classical Cepheids could be detected in both H- and K_s-band images in our survey. Solid and dashed curves indicate saturation and fainter limits, for each of which, curves corresponding to three different periods of Cepheids, i.e. different absolute magnitudes, are drawn. Three-dimensional extinction map by Schultheis et al. (2014), A_{K_s} increasing as a function of distance, is illustrated by the thick dotted curve and the shaded area; the former indicates the median curve of A_{K_s} values along the lines of sight towards 142 IRSF/SIRIUS fields-of-view in our survey and the latter shows the range of 90 percentile at each distance.

solid curves in Fig. 3 in order to be detected in our survey. With $A_{K_s} = 2.5$, for example, Cepheids with $\log P = 0.7$ are around the detection limit at the distance of ∼8 kpc, while those with $\log P > 1.0$ can be detected at a significantly larger distance. It is therefore possible to detect longer period Cepheids within several kpc, both on the nearer and on the further side, around the Galactic Centre unless the extinction gets significantly larger. The lack of our detection of such Cepheids indicates the absence of Cepheids in the corresponding region.

We found no classical Cepheids significantly closer than the four in the Galactic Centre although there seems to be room in the parameter space in which Cepheids could have been detected in our survey. The three-dimensional extinction map by Schultheis et al. (2014) suggests that the extinction remains smaller than 0.5 mag in A_{K_s} up to ∼3.5 kpc (Fig. 3). With such an extinction at the smaller distance, even short-period Cepheids must have been saturated. No such Cepheids, if any, in our survey field have been reported in previous variability catalogues (DDO Database of Galactic Classical Cepheids, Fernie et al. 1995; General Catalogue of Variable Stars, Samus et al. 2015; AAVSO International Variable Star Index, Watson, Henden & Price 2015).

In the range of 3.5–6 kpc in distance, some Cepheids could have been detected in our survey depending on the period and the foreground extinction. This range corresponds to the Galactocentric distance of 2–4.5 kpc with the Galactic Centre distance assumed to be 8 kpc, thus in the vicinity of the 3 kpc arm and closer to the Centre. Our survey field, ∼2.3 deg², covers 0.04 kpc³ in this distance range along the Galactic mid-plane. The DDO Database (Fernie et al. 1995) lists 71 Cepheids within 2 kpc around the Sun and within 50 pc of the Galactic plane, which gives a volume density of 110 kpc⁻³. Assuming the density gets higher towards the inner region following an exponential law with a scale length of 3.5 kpc (see Windmark, Lindegren & Hobbs 2011), the density in the above volume would be higher by a factor of ∼3, thus leading to ∼350 kpc⁻³. This suggests that about 14 Cepheids could be included within our survey field at 3.5–6 kpc, although we found none.

In order to take the completeness of our survey into account, we made a Monte Carlo simulation as follows. First, we generate 5000 Cepheids uniformly distributed within our survey volume between 3.5 and 6 kpc. Then, we assign their periods randomly but following the period distribution of the DDO Database Cepheids in the solar neighbourhood (see fig. 2 of Matsunaga et al. 2011). With the PLRs (equations 1 and 2) and the extinction from the map by Schultheis et al. (2014) for each simulated Cepheid, we can calculate its expected magnitudes in H and K_s and determine whether it would be detected in our survey or not. The simulation suggests that ∼70 per cent of Cepheids located in this volume should have been detected. Considering the space density mentioned above, we could have detected about 10 Cepheids in our survey with the assumed space distribution. The absence of such Cepheids indicates that the density of Cepheids in the inner part of the disc, except the NSD, is lower than expected by the simple exponential law. The volume density in the inner part may be even smaller than that in the solar neighbourhood with which ∼3 Cepheids are expected to be found in our survey.

4.3 Distribution of Cepheids across the Galactic plane

Fig. 4 plots the distribution of our Cepheids and Dékány's sample by filled and open circles. Locations of the DDO Database Cepheids are indicated by grey points (e.g. see Majaess, Turner & Lane, 2009,
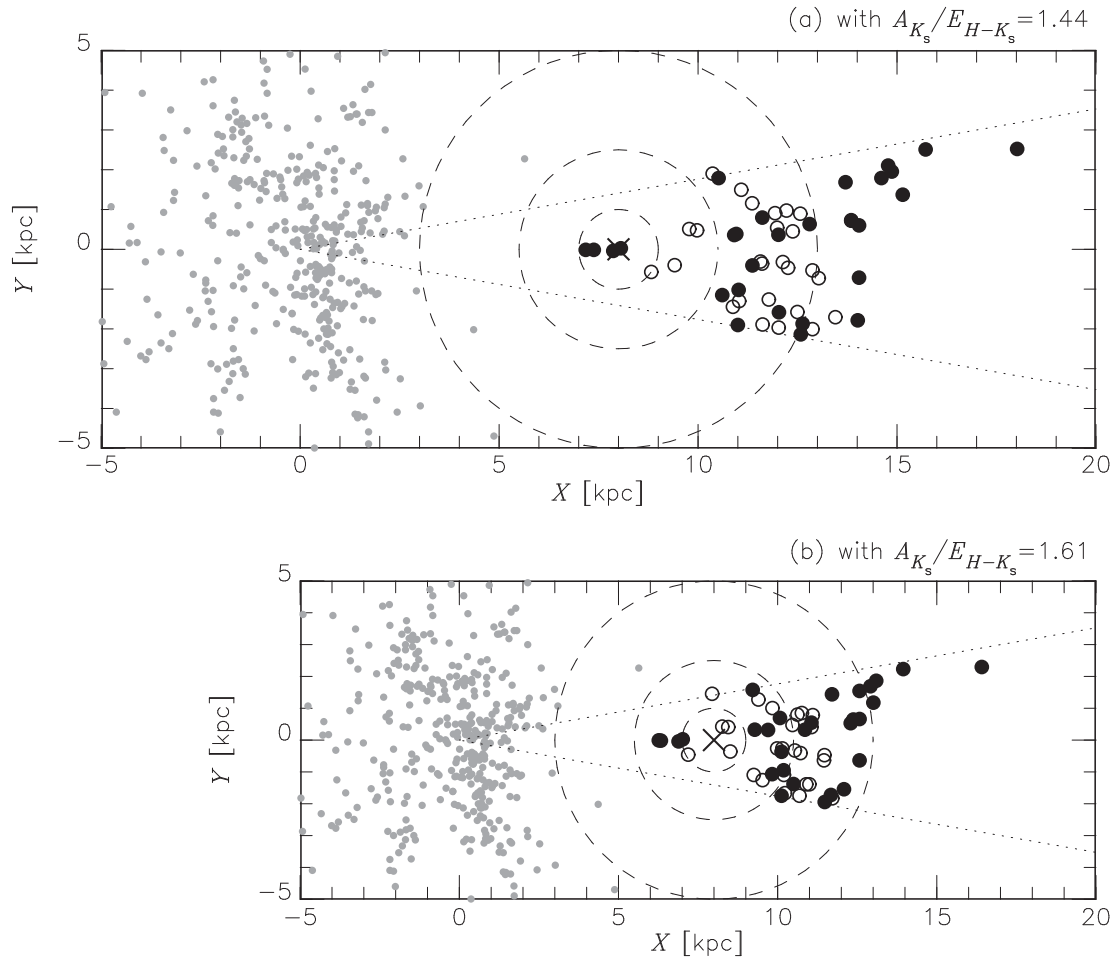
Figure 4. Distribution of Cepheids, ours and those in Dékány et al. (2015a,b) indicated by filled and open circles, respectively, on the face-on view of the Galactic disc. The reddening law by Nishiyama et al. (2006) was used for both sample in the panel (a), while that by Nishiyama et al. (2009) was used in the panel (b). Note the displacement of the four NSD Cepheids from the Centre in (b). If a Cepheid is found in both surveys, a distance obtained with our photometry is used. Grey points show the distribution of previous Cepheids in Fernie et al. (1995). The Sun is located at the origin, and the Galactic Centre is indicated by the cross at an assumed distance of 8 kpc. Dashed circles at 1, 2.5 and 5 kpc from the Galactic Centre are drawn for readers' convenience. The longitude range of our survey, $|l| < 10°$, is illustrated by dotted lines.

for discussions on their distribution). Here, again, the distances of the Dékány's objects are obtained based on our adopted PLR and the extinction law of Nishiyama et al. (2006). Except the four Cepheids belonging to the NSD, none of our Cepheids, indicated by filled circles, are within 2.5 kpc around the Galactic Centre indicated by the cross. Therefore, we found no evidence of the disc-like distribution of young stars in the inner part of the Galaxy suggested by Dékány et al. (2015b), except the NSD.

Towards the bulge but in regions of higher Galactic latitude, $|b| > 2°$, Soszyński et al. (2011) reported 32 classical Cepheids found in the Optical Gravitational Lensing Experiment (OGLE). The apparent magnitudes of these Cepheids are similar to those of type II Cepheids in the bulge (fig. 7 in Soszyński et al. 2011), and thus, if these are indeed classical Cepheids, they are expected to be significantly further than the bulge. Five of them are confirmed to be classical Cepheids located in the flared part of the disc by Feast et al. (2014), while accurate distances and natures of the others are not well determined. The five Cepheids in Feast et al. (2014) are located outside the range of Fig. 4, at heliocentric distances of 22 kpc or larger. Their distances from the Galactic plane, >1 kpc, are also distinctly larger than the Cepheids plotted in Fig. 4.

Among the Cepheids reported by Dékány's et al., four stars (their 11, 13, 20 and 22) are relatively close to the Galactic Centre, 1–2 kpc. Unfortunately, none of them is within our survey field. Their exact locations and kinematics are of great interest to study stellar populations of the inner part of the Galaxy.

On the other hand, as we discussed in Section 4.2, we found no Cepheids closer than the four immediately around the Galactic Centre. In addition, there seems to be a space, at the Galactic distance of 2.5–5 kpc, without any Cepheids on the nearer side of the Galactic Centre in contrast to the further side where dozens Cepheids were found (Dékány et al. 2015a,b and this work). Our survey only partly covers this relatively close range (3–5.5 kpc from the Sun) due to the saturation limit (Fig. 3). Previous surveys may also have been incomplete in this region since our survey and that of Dékány et al. (2015a,b) have found Cepheids at the corresponding Galactocentric distance on the opposite side of the Centre. Deeper and more comprehensive surveys in the optical, such as *Gaia*, or shallower surveys in the infrared will have the capability to provide a more complete mapping of variable star populations.

5 CONCLUDING REMARKS

The presence of an inner thin disc, represented by Cepheids, which was suggested by Dékány et al. (2015b) has not been confirmed. The lack of Cepheids in the inner part of the Galaxy, a few kpc both on the front- and far-side of the Galactic Centre, suggests that the young stellar populations do not follow the exponential disc distribution towards the centre. A similar lack in the inner disc has been also found in the distribution of H II regions. Our study demonstrated that the extinction law has a strong impact on investigations of the distribution of obscured stars in the inner Galaxy. It is nonetheless clear that the recent infrared surveys are revealing populations of Cepheids in a large area of the Galaxy, including the opposite side of the disc beyond the bulge. Detailed observations of these objects, such as high-resolution spectroscopy for radial velocities and metallicities, would provide a new path to a global picture of Galactic structure and evolution.

ACKNOWLEDGEMENTS

REFERENCES

Anderson L. D., Bania T. M., Balser D. S., Rood R. T., 2011, ApJS, 194, 32
Anderson L. D., Bania T. M., Balser D. S., Rood R. T., 2012, ApJ, 754, 62
Benedict G. F. et al., 2007, AJ, 133, 1810
Bono G., Marconi M., Cassisi S., Caputo F., Gieren W., Pietrzynski G., 2005, ApJ, 621, 966
Chen B. Q., Schultheis M., Jiang B. W., Gonzalez O. A., Robin A. C., Rejkuba M., Minniti D., 2013, A&A, 550, A42
Dame T. M., Thaddeus P., 2008, ApJ, 683, L143
Dékány I. et al., 2015a, ApJ, 799, L11
Dékány I. et al., 2015b, ApJ, 812, L29
Feast M. W., Menzies J. W., Matsunaga N., Whitelock P. A., 2014, Nature, 509, 342
Fernie J. D., Evans N. R., Beattie B., Seager S., 1995, Inf. Bull. Var. Stars, 4148, 1
Figer D. F., McLean I. S., Morris M., 1999, ApJ, 514, 202
Figer D. F. et al., 2002, ApJ, 581, 258
Fritz T. K. et al., 2011, ApJ, 737, 73
Gillessen S., Eisenhauer F., Fritz T. K., Pfuhl O., Ott T., Genzel R., 2013, in de Grijs R., ed., Proc. IAU Symp. 289, Advancing the Physics of Cosmic Distances. Cambridge Univ. Press, Cambridge, p. 29
Gosling A. J., Bandyopadhyay R. M., Blundell K. M., 2009, MNRAS, 394, 2247
Jones C., Dickey J. M., Dawson J. R., McClure-Griffiths N. M., Anderson L. D., Bania T. M., 2013, ApJ, 774, 117
Launhardt R., Zylka R., Mezger P. G., 2002, A&A, 384, 112
Majaess D. J., Turner D. G., Lane D. J., 2009, MNRAS, 398, 263
Matsunaga N., 2014, EAS Publ. Ser., 67, 279
Matsunaga N., Kawadu T., Nishiyama S., Nagayama T., Hatano H., Tamura M., Glass I. S., Nagata T., 2009, MNRAS, 399, 1709
Matsunaga N. et al., 2011, Nature, 477, 188
Matsunaga N. et al., 2013, MNRAS, 429, 385
Matsunaga N. et al., 2015, ApJ, 799, 46
Mauerhan J. C., Cotera A., Dong H., Morris M. R., Wang Q. D., Stolovy S. R., Lang C., 2010, ApJ, 725, 188
Minniti D. et al., 2010, New Astron., 15, 433
Monson A. J., Fredman W. L., Madore B. F., Persson S. E., Scowcroft V., Seibert M., Rigby J. R., 2012, ApJ, 759, 146
Nagashima C. et al., 1999, in Nakamoto T., ed., Proc. Star Formation 1999. Nobeyama Radio Observatory, Nagano, p. 397
Nagayama T. et al., 2003, in Iye M., Moorwood A. F. M., eds, Proc. SPIE Vol. 4841, Instrument Design and Performance for Optical/Infrared Ground-Based Telescopes. SPIE, Bellingham, p. 459
Nataf D. M. et al., 2013, ApJ, 769, 88
Nishiyama S. et al., 2005, ApJ, 621, L105
Nishiyama S. et al., 2006, ApJ, 638, 839
Nishiyama S., Tamura M., Hatano H., Kato D., Tanabé T., Sugitani K., Nagata T., 2009, ApJ, 696, 1407
Pietrzyński G. et al., 2013, Nature, 495, 76
Rattenbury N. J., Mao S., Sumi T., Smith M. C., 2007, MNRAS, 378, 1064
Saito R. K., Zoccali M., McWilliam A., Minniti D., Gonzalez O. A., Hill V., 2011, AJ, 142, 76
Samus N. N., Durlevich O. V., Goranskij V. P., Kazarovets E. V., Kireeva N. N., Pastukhova E. N., Zharova A. V., 2015, General Catalogue of Variable Stars, VizieR On-line Data Catalog: B/gcvs
Sanna A. et al., 2014, ApJ, 781, 108
Schödel R., Najarro F., Muzic K., Eckart A., 2010, A&A, 511, A18
Schultheis M. et al., 2014, A&A, 566, A120
Soszyński I. et al., 2011, Acta Astron., 61, 285
van Leeuwen F., Feast M. W., Whitelock P. A., Laney C. D., 2007, MNRAS, 379, 723
Watson C., Henden A. A., Price A., 2015, AAVSO International Variable Star Index, VizieR On-line Data Catalog: B/vsx
Wegg C., Gerhard O., 2013, MNRAS, 435, 1874
Windmark F., Lindegren L., Hobbs D., 2011, A&A, 530, A76
Yusef-Zadeh F. et al., 2009, ApJ, 702, 178

This paper has been typeset from a TEX/LATEX file prepared by the author.